ACS Catalysis

Research Article

pubs.acs.org/acscatalysis

Volcano-Curves for Dehydrogenation of 2-Propanol and Hydrogenation of Nitrobenzene by SiO_2-Supported Metal Nanoparticles Catalysts As Described in Terms of a d-Band Model

Masazumi Tamura,[†] Kenichi Kon,[‡] Atsushi Satsuma,[§] and Ken-ichi Shimizu*[,‡]

[†]Department of Applied Chemistry, School of Engineering, Tohoku University, 6-6-07, Aoba, Aramaki, Aoba-ku, Sendai 980-8579, Japan

[‡]Catalysis Research Center, Hokkaido University, N-21, W-10, Sapporo 001-0021, Japan

[§]Department of Molecular Design and Engineering, Graduate School of Engineering, Nagoya University, Furo-cho, Chikusa-ku, Nagoya 464-8603, Japan

Supporting Information

ABSTRACT: To confirm whether the activity trends in multistep organic reactions can be understood in terms of the Hammer–Nørskov d-band model in combination with the linear energy relations, we studied correlations between the reaction rates for dehydrogenation and hydrogenation reactions and the position of the d-band center (ε_d) relative to the Fermi energy (E_F), the $\varepsilon_d - E_F$ value, of various metal catalysts. SiO_2-supported metal (M = Ag, Cu, Pt, Ir, Pd, Rh, Ru, Ni, and Co) catalysts with the same metal loading (5 wt %) and similar metal particle size (8.9–11.7 nm) were prepared. The dehydrogenation of adsorbed 2-propanol in a flow of He and the hydrogenation of adsorbed nitrobenzene in a flow of H_2 were tested as model reactions of organic reactions on the metal surface. As a test reaction of H_2 dissociation on the surface, SiOH/SiOD exchange on the M/SiO_2 catalysts in a flow of D_2 is carried out. The liquid phase hydrogenation of nitrobenzene under 3.0 MPa of H_2 is adopted as an organic reaction under realistic conditions. Generally, the activities show volcano-type dependences on the $\varepsilon_d - E_F$ value, indicating that the $\varepsilon_d - E_F$ value is useful as a qualitative activity descriptor in heterogeneous catalysis of metal nanoparticles for multistep organic reactions.

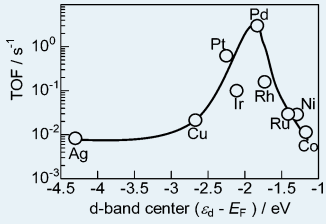

KEYWORDS: *transition metals, trend in catalytic activity, d-band center*

INTRODUCTION

Prediction of a trend in the catalytic activity from the electronic structure of metals is one of the long-term goals of catalysis research because this would open possibilities in the design of surfaces with specific catalytic properties without extensive trial-and-error experimental testing. To predict catalytic activity, parameters correlated with catalytic activity should be clarified. For a reaction involving a bond dissociation of reactants on metal surfaces, activities have been correlated with bond energy derived from bulk oxide properties or various atomic or molecular chemisorption energies.[1] Empirically, a volcano-shaped curve is often obtained when the activity of catalysts for a certain reaction is plotted as a function of these parameters. For a specific reaction, strong binding of an intermediate may lead to surface poisoning, whereas weak binding may lead to limited availability of the intermediate; in both cases, catalytic rates are less than optimal. Consequently, a moderate interaction leads to the highest reactivity (the principle of Sabatier). Although the concept of the volcano curve is useful as a guideline in the research for new catalysts, there is a problem of finding systematic databases of relevant surface thermo-chemical data. Recently, a linear relationship between the activation energy and the adsorbate–surface interaction energy, known as the Brønsted–Evans–Polanyi relation, has been found by several groups using theoretical calculations, which makes it possible to quantitatively understand the volcano curve in heterogeneous catalytic systems.[2−15]

Using the density functional theory (DFT) calculations as computer experiments, Nørskov and co-workers[2−5,16−18] have systematically studied which parameters influence the reactivity of the metal surface. On the basis of the assumption that the d electrons of transition metals play the most important role in chemisorption, a summary of many calculations has led to a semiempirical concept, so-called the d-band model. This model provides linear scaling between the energy of the d-band center (ε_d) relative to the Fermi level (E_F) and adsorption energy for a given adsorbate. The higher the d-states are in energy relative to the Fermi level, the more empty the antibonding states and the stronger the adsorption bond. The calorimetric study by Lu et al.[19] gave experimental evidence to support the d-band model; they showed moderately linear correlations between the experimental heat of adsorption of CO, H_2, O_2, C_2H_4 on various metal surfaces and the position of the d-band center calculated by Nørskov et al.[2] The d-band model also show that adsorbate binding energies should be correlated with each other.[4] Since the transition-state structures over different metals

Received: June 12, 2012
Revised: July 24, 2012
Published: July 27, 2012

tend to be rather similar, the activation energy for an elementary reaction can be linearly correlated to the energy change for the elementary reaction. Thus, the kinetic parameter for a catalytic reaction by a particular metal can be described by a single parameter, $\varepsilon_d - E_F$, the position of d-band center relative to E_F. Actually, several electrochemical studies showed a correlation between the catalytic activity for the oxygen reduction reaction and the position of d-band center, which led to the discovery of new electrocatalysts.[18,20,21] However, the applicability of the d-band model to conventional heterogeneous catalysis, such as dehydrogenation and hydrogenation, has been mostly supported by the correlation between calculated $\varepsilon_d - E_F$ values and calculated thermo-chemical or kinetic parameters.[2−5,15−17,22] For example, Pallassana and Neurock showed a linear correlation between the d-band center and the calculated activation energies of ethylene hydrogenation over various metal surfaces.[22] Recently, Chen and coworkers[23] determined interaction energies between metal surfaces and propanol on Ni−Pt, Pt, and Ni surfaces as well as kinetic parameters for hydrogenation of propanal and showed correlations between calculated d-band center and experimentally determined thermo-chemical and kinetic parameters.

To confirm experimentally whether the activity trends in multistep organic reactions can be understood in terms of the d-band model in combination with the linear energy relations, we studied correlations between the reaction rates for dehydrogenation and hydrogenation reactions and the $\varepsilon_d - E_F$ values. The dehydrogenation of 2-propanol and hydrogenation of nitrobenzene by H_2 were chosen as test reactions. To minimize the effects of diffusion and surface coverage, a small amount of the reactant was subjected to the catalyst inside the in situ IR cell, and we measured the initial rate for the dehydrogenation of adsorbed 2-propanol in a flow of He and those for the hydrogenation of adsorbed nitrobenzene in a flow of H_2. As a test reaction of H_2 dissociation on the surface, OH/OD exchange on the SiO_2 surface in a flow of D_2 was carried out. We also tested the liquid phase hydrogenation of nitrobenzene under 3.0 MPa of H_2 to study whether the $\varepsilon_d - E_F$ value is sufficient for a semiquantitative parameter of multistep organic reactions under realistic conditions.

EXPERIMENTAL SECTION

General Procedures. Commercially available organic and inorganic compounds were used without further purification. Aqueous HNO_3 solution of $Pt(NH_3)_2(NO_3)_2$, $Rh(NO_3)_3$, and $Pd(NO_3)_2$, nitrates of Co(II), Ni(II), Cu(II), and Ag(I), chloride hydrates of Ru(III) and Ir(III) were used in the catalyst preparation. The GC (Shimadzu GC-14B) and GCMS (Shimadzu GCMS-QP5000) analyses were carried out with Rtx-65 capillary column (Shimadzu) using nitrogen as the carrier gas. Powder X-ray diffraction (XRD) patterns were acquired on MiniFlex II (Rigaku) with Cu Kα radiation. Transmission electron microscopy (TEM) measurements were investigated by using a JEOL JEM-2100F TEM operated at 200 kV.

Catalyst Preparation and Characterization. SiO_2-supported metal (M = Ag, Cu, Pt, Ir, Pd, Rh, Ru, Ni, and Co) catalysts (M/SiO_2 with M loading of 5 wt %) were prepared by impregnating SiO_2 (Q-10, 300 $m^2\ g^{-1}$, supplied from Fuji Silysia Chemical Ltd.) with an aqueous solution of each metal salts, followed by evaporation to dryness at 80 °C, drying at 100 °C for 12 h, calcination in air for 1 or 3 h, and reduction in H_2. To control the metal particle size, calcination condition and reduction condition were changed as summarized in Table 1. Catalysts were pretreated by oxidation at T_{H2} in 10% O_2/He flow (100 mL min^{-1}) for 10 min and reduction at T_{H2} in 2% H_2/He flow (100 mL min^{-1}) for 10 min before using them for the reaction.

Table 1. List of Catalysts

Catalysts	T_{cal}/°C[a]	T_{H2}/°C[b]	D/nm[c]
Co/SiO_2	500	500[e]	9.3 ± 2.0
Ni/SiO_2	500	500[d]	10.6 ± 2.2
Cu/SiO_2	100	250[d]	11.7 ± 2.7
Ru/SiO_2	500	500	9.3 ± 1.7
Rh/SiO_2	900	500	11.2 ± 2.7
Pd/SiO_2	700	200	10.0 ± 2.2
Ag/SiO_2	500	500	8.9 ± 1.9
Ir/SiO_2	100	500	10.0 ± 2.2
Pt/SiO_2	700	200	11.5 ± 2.7

[a]Temperature of calcination. [b]Temperature of reduction in H_2/He. [c]The volume-area mean diameter of metal particles estimated by TEM. [d]In a flow of 100% H_2. [e]Reduction time was 20 min.

In the XRD patterns of M/SiO_2 catalysts, diffraction lines due to metal oxides were not observed, but lines due to metallic phase were observed. The metal particle distribution for each catalyst is shown in the Supporting Information, Figure S1. It is known that the mean particle diameter estimated from the number of surface atoms on the assumption of spherical particles agrees with a volume-area mean diameter measured by TEM.[24] Hence, the volume-area mean diameter is calculated as shown in Table 1. The mean diameter of the particle size was in a range of 8.9 to 11.7 nm. Consequently, a series of M/SiO_2 catalysts with the same loading (5 wt %) and similar metal particle size (8.9−11.7 nm) were prepared as listed in Table 1.

Surface Reactions Monitored by in Situ FTIR. In situ FTIR spectra were recorded by a JASCO FT/IR-6100 equipped with a quartz IR cell connected to a conventional flow reaction system. The sample was pressed into a 15−30 mg of self-supporting wafer and mounted into the quartz IR cell with CaF_2 windows. Spectra were measured accumulating 15 scans at a resolution of 4 cm^{-1}. A reference spectrum of the catalyst wafer in He was subtracted from each spectrum. Prior to each experiment the catalyst disk was pretreated under the condition shown in Table 1, followed by cooling to reaction temperature under He flow. For the introduction of 2-propanol and nitrobenzene to the IR disk, the liquid compound was injected under the He flow preheated at 150 °C which was fed to the in situ IR cell. Extinction coefficient of adsorbed 2-propanol was determined by IR band area of adsorbed 2-propanol on SiO_2 at 30 °C and the amount of adsorbed 2-propanol. The latter value was calculated from the amount of 2-propanol introduced to the IR cell and that of outlet monitored by online mass spectroscopy. The band area increased linearly with the amount of adsorbed 2-propanol, and the integrated molar extinction coefficient was calculated using the slope of the line and the Lambert−Beer law.

Liquid Phase Hydrogenation of Nitrobenzene. Hydrogenation of nitrobenzene was carried out in a 30 cm^3 autoclave with a glass tube inside equipped with magnetic stirring. Nitrobenzene (2 mmol) and tetrahydrofuran (15 cm^3) were placed into the autoclave together with typically 0.05−0.4 mol % of catalyst pretreated under the condition shown in Table 1.

dx.doi.org/10.1021/cs300376u | ACS Catal. 2012, 2, 1904−1909

After being sealed, the reactor was flushed with H_2 and pressured at 3.0 MPa, and then heated to 100 °C. Conversion and yields of products were determined by GC using *n*-dodecane as an internal standard. The products were identified by gas chromatography/mass spectroscopy (GC-MS-QP500, Shimadzu) equipped with same column and in the same conditions as GC and also by comparison with commercially pure products.

RESULTS

Dehydrogenation of Adsorbed 2-Propanol. The dehydrogenation of adsorbed 2-propanol on M/SiO_2 was tested by in situ IR at 30 °C in a flow of He. Figure 1A shows

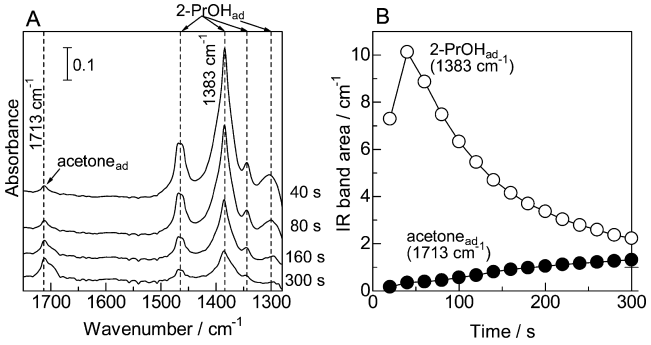

Figure 1. (A) Changes in IR spectra and (B) area of IR bands vs time for dehydrogenation of adsorbed 2-PrOH on Rh/SiO_2 under a flow of He at 30 °C.

changes in the spectra of adsorbed species on Rh/SiO_2 as a function of time after the introduction of 2-propanol (2 μL) to the catalyst disk. Initially (t = 40 s), IR bands due to adsorbed 2-propanol (2-PrOH$_{ad}$) were observed at 1465, 1384, 1344, and 1300 cm^{-1}.[25] The presence of the band at 1300 cm^{-1} due to OH deformation of 2-propanol indicates that 2-PrOH$_{ad}$ is not a 2-propoxide species but a nondissociatively adsorbed 2-propanol species on the catalyst. Then, the intensities of the band due to 2-PrOH$_{ad}$ decreased with time. Simultaneously, a new band at 1713 cm^{-1} due to C═O stretching of adsorbed acetone appeared. In contrast, 2-PrOH$_{ad}$ on SiO_2 was relatively stable, and it did not convert to acetone (not shown). This suggests that the Rh metal particle on Rh/SiO_2 catalyzes the dehydrogenation of 2-PrOH$_{ad}$ to acetone. The area of the band at 1384 cm^{-1} is plotted as a function of time in Figure 1B. Using the initial slope of the kinetic curve and the adsorption coefficients of 2-PrOH$_{ad}$ (1.63 cm μmol^{-1}) experimentally determined, we estimated the initial rate of the 2-PrOH$_{ad}$ dehydrogenation on Rh/SiO_2 (0.124 mmol s^{-1} g_{Rh}^{-1}). By using the mean diameter of Rh metal particle (7.9 nm) shown in Table 1 and the atomic diameter of Rh (0.278 nm) and assuming that the supported Rh particles can be modeled as a fcc crystal lattice with a cuboctahedral shape, the number of surface Rh atoms was determined according to the established method.[26] This value was then used to estimate turnover frequency (TOF) per surface Rh atom shown in Figure 2. For a series of the M/SiO_2 catalysts (M = Co, Ni, Cu, Ru, Rh, Pd, Ag, Ir, and Pt), the same experiment was carried out, and the TOF values were estimated as summarized in Figure 2. The activity changed in the following order: Pt/SiO_2 > Ir/SiO_2 > Rh/SiO_2 > Ni/SiO_2 > Ru/SiO_2 > Ag/SiO_2 > Co/SiO_2 > Cu/SiO_2 > Pd/SiO_2.

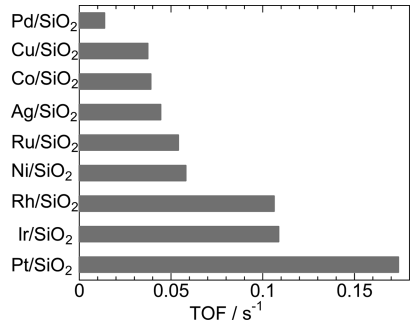

Figure 2. TOF for dehydrogenation of 2-PrOH adsorbed on M/SiO_2 at 30 °C.

Hydrogenation of Adsorbed Nitrobenzene. Hydrogenation of adsorbed nitrobenzene was also studied by in situ IR at 50 °C. Nitrobenzene (1 μL) was injected to the catalyst disk under a He flow which was fed to the in situ IR cell, followed by purging the IR cell with He until the band was stable. Then, in situ IR spectra measurement was carried out in a flow of H_2 under normal pressure. Figure 3A shows changes

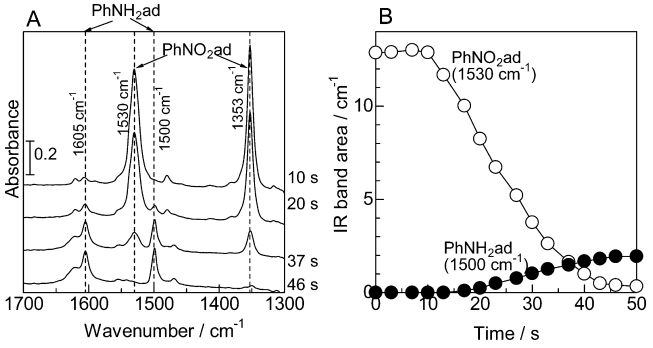

Figure 3. (A) Changes in IR spectra and (B) area of IR bands vs time for hydrogenation of adsorbed $PhNO_2$ on Rh/SiO_2 under a flow of H_2 at 50 °C.

in the spectra of adsorbed species on Rh/SiO_2 versus time of H_2 flowing. At t = 0 s (before the H_2 feed), IR bands due to the $\nu_{as}(NO_2)$ and $\nu_s(NO_2)$ of the adsorbed nitrobenzene (PhNO$_{2ad}$)[27] were observed at 1353 and 1530 cm^{-1}, respectively. When the flowing gas was switched to H_2, the band intensity for PhNO$_{2ad}$ decreased with time and nearly disappeared at t = 50 s. Simultaneously, new bands due to adsorbed aniline (1500 and 1605 cm^{-1})[27] appeared, and their intensities increased with time. In contrast, nitrobenzene adsorbed on SiO_2 did not react under the same condition. These results indicate that SiO_2 does not participate in hydrogenation of nitrobenzene. The kinetic curves for the PhNO$_{2ad}$ consumption and aniline formation over Rh/SiO_2 are shown in Figure 3B. The IR intensity of PhNO$_{2ad}$ and aniline were estimated from the area of the IR bands at 1530 cm^{-1} and 1605 cm^{-1}, respectively. The intensity of the band at 1530 cm^{-1} due to PhNO$_{2ad}$ on Rh/SiO_2 did not decrease under a flow of He (not shown), which indicates that PhNO$_{2ad}$ was a stable adspecies under a flow of inert gas. From the slope of the straight line of the kinetic curve, the adsorption coefficients of nitrobenzene (7.56 cm μmol^{-1}),[28] and the number of surface Rh atoms estimated from the average size of Rh metal particles, TOF for the consumption of nitrobenzene under H_2 was estimated. The same experiment was carried out with other

dx.doi.org/10.1021/cs300376u | ACS Catal. 2012, 2, 1904−1909

catalysts. TOFs for hydrogenation of $PhNO_{2ad}$ on M/SiO_2 are shown in Figure 4. The order of catalytic activity was as follows: Pd/SiO_2 > Pt/SiO_2 > Rh/SiO_2 > Ir/SiO_2 > Ag/SiO_2 > Ru/SiO_2 > Cu/SiO_2 > Ni/SiO_2 > Co/SiO_2.

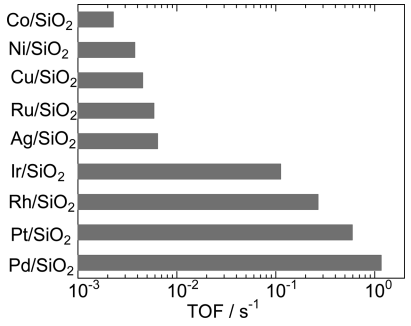

Figure 4. TOF for hydrogenation of $PhNO_2$ adsorbed on M/SiO_2 under H_2 at 50 °C.

OH/OD Exchange under D_2. As reported by Claus and co-workers for Ag/SiO_2 catalysts,[29] the isotopic exchange of OH groups of SiO_2 to OD groups in D_2 begins with the cleavage of D_2, and thus, this reaction can be considered a model reaction for measuring the rate of the D_2 dissociation according to the method in our previous study.[25] Figure 5A shows the IR spectra

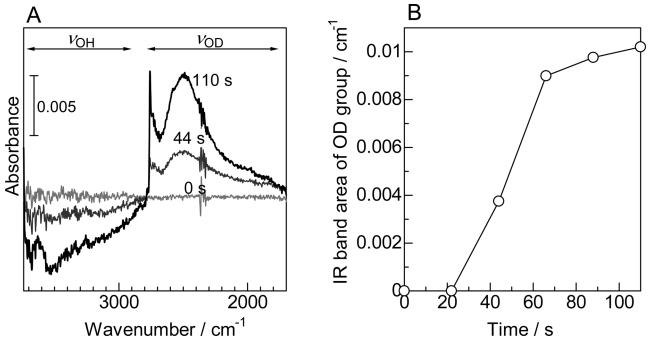

Figure 5. (A) Changes in IR spectra and (B) area of IR bands vs time for the H/D exchange of surface SiOH groups of Rh/SiO_2 under a flow of D_2 at 30 °C.

as a function of time of D_2 flowing to Rh/SiO_2 at 30 °C. Loss and gain of IR band intensity in the SiO-H (2800−3800 cm^{-1}) and in the SiO−D (1900−2800 cm^{-1}) stretching regions were observed, indicating the OH/OD exchange of the surface SiOH groups. Kinetic curves for the OD formation are shown in Figure 5B. From the slope of the initial straight line of the kinetic curve and weight of the IR disk, a relative rate for the OD formation under D_2 was estimated. The results for various M/SiO_2 catalysts are shown in Figure 6. The D_2 dissociation rate changed in the following order: Pt/SiO_2 > Ir/SiO_2 > Rh/SiO_2 > Pd/SiO_2 > Ag/SiO_2 > Cu/SiO_2 > Ru/SiO_2 > Co/SiO_2 > Ni/SiO_2.

Hydrogenation of Nitrobenzene in the Batch Reaction System. The liquid phase hydrogenation of nitrobenzene was examined in THF under 3 MPa H_2 with M/SiO_2 catalysts at 100 °C (Table 2). TOF was calculated using the rate and the metal particle size in Table 1. The order of catalytic activity was as follows; Pd/SiO_2 > Pt/SiO_2 > Rh/SiO_2 > Ir/SiO_2 > Ru/SiO_2 > Ni/SiO_2 > Cu/SiO_2 > Co/SiO_2 > Ag/SiO_2 (Figure 7).

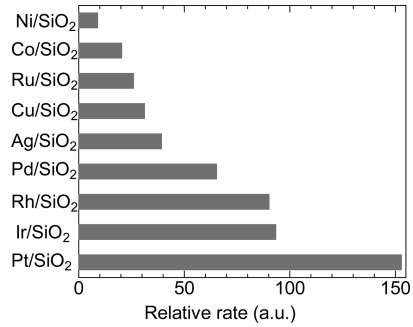

Figure 6. Initial rate for the H/D exchange of surface SiOH groups of M/SiO_2 under D_2 at 30 °C.

Table 2. Liquid Phase Hydrogenation of Nitrobenzene

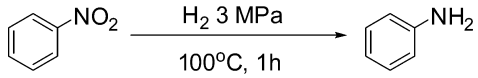

catalyst (mg)[a]	conv. (%)	yield (%)	TOF/s^{-1}
Pd/SiO_2 (2.1)	77	74	3.0
Pt/SiO_2 (1.0)	6.3	3.6	0.61
Rh/SiO_2 (1.9)	3.6	3.4	0.16
Ir/SiO_2 (3.9)	3.2	2.3	0.10
Ni/SiO_2 (35)	19	17	0.03
Ru/SiO_2 (27)	23	9.7	0.03
Cu/SiO_2 (28)	8.7	8.6	0.02
Co/SiO_2 (36)	8.5	7.9	0.01
Ag/SiO_2 (42)	5.4	4.6	0.008

[a]Catalyst loading (mg).

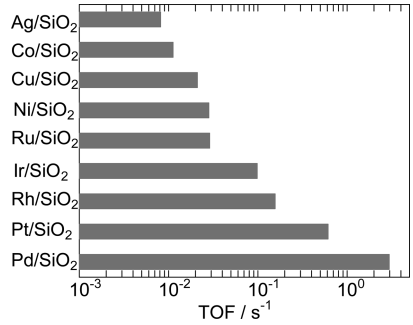

Figure 7. TOF for liquid phase hydrogenation of $PhNO_2$ by M/SiO_2 under H_2 (3.0 MPa) at 100 °C.

DISCUSSIONS

To discuss the reactivity order of the different transition metal catalysts in terms of the Hammer−Nørskov d-band model, TOF for various metal-loaded SiO_2 are plotted in Figure 8 as a function of the d-band center (ε_d) relative to the Fermi energy (E_F) for the clean metal surface. Note that the metal particle sizes of M/SiO_2 catalysts are relatively large (8.9−11.7 nm), which indicates that majority of the surface metal atoms are at plane sites. Thus, we used the average energy of d-states (ε_d) projected on the surface atom on the most close packed surface calculated by Nørskov and co-workers.[2,16] For the dehydrogenation of 2-PrOH_{ad} on M/SiO_2 (Figure 8A), hydrogenation of $PhNO_{2ad}$ on M/SiO_2 (Figure 8B), OH/OD exchange of surface SiOH groups under D_2 on M/SiO_2(Figure 8C), and liquid phase hydrogenation of $PhNO_2$ by M/SiO_2 (Figure 8D), the activities generally show volcano-type dependences on the ε_d-E_F value, except for the Pd catalyst in Figure 8A.

dx.doi.org/10.1021/cs300376u | ACS Catal. 2012, 2, 1904−1909

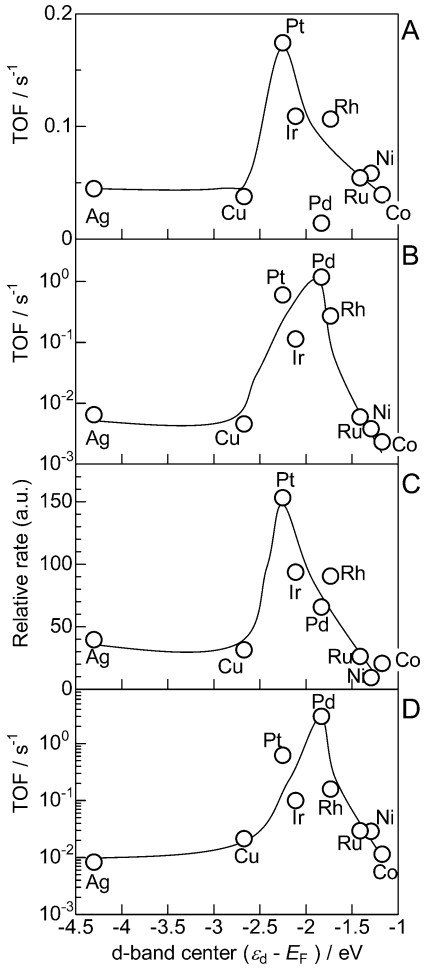

Figure 8. TOF for (A) dehydrogenation of 2-$PrOH_{ad}$ at 30 °C, (B) hydrogenation of $PhNO_{2ad}$ at 50 °C, (C) H/D exchange of surface SiOH groups under D_2 on M/SiO_2 at 30 °C, and (D) liquid phase hydrogenation of $PhNO_2$ by M/SiO_2 at 100 °C as a function of the d-band center of metals (ε_d) relative to the Fermi energy (E_F).

There is a generally observed tendency that the further the d-band center is from E_F the weaker the metal−hydrogen (M-H) and metal−oxygen (M-O) bond energies.[17] As shown in Supporting Information, Figure S2, we confirmed moderate correlations between the d-band center and the M-H and M-O bond energies calculated by Toulhoat and Raybaud.[8] Note that all the reactions in Figure 8 include the formation and dissociation of M-H bonds as a common elementary step. Dehydrogenation and hydrogenation reactions include the formation and dissociation of M-O bonds. Hence, the result in Figure 8 suggests that the moderate M-H and/or M-O bond strength is favorable for these reactions. However, replotting the activity patterns with respect to the calculated M-H (Supporting Information, Figure S3) and M-O (Supporting Information, Figure S4) bond energies[8] gave relatively poor correlations. It follows that the d-band center is the most convenient activity descriptor for the catalytic systems tested in this study. A possible explanation of this result is as follows. Strong binding of surface intermediates via M-H and M-O bonds lead to surface poisoning, whereas weak binding of the intermediates lead to limited availability of the intermediate; in both cases, catalytic rates are less than optimal. Consequently, platinum-group-metal catalysts with moderate bond strength gave highest activity. Both M-H and M-O bond energies can influence the rate of elementary steps as well as surface coverage of the intermediates. This may be why the M-H and M-O bond energies were poorer activity descriptors than the d-band center as an averaged parameter of metal-adsorbate interaction energies.

Although the d-band model suggests that the reactivity of a particular metal catalyst may be described by a single parameter, $\varepsilon_d - E_F$, there are quite a few experimental studies that verify the applicability of this semiempirical concept to transition metal catalyzed multistep organic reactions.[23] The above results demonstrate that the d-band model (in combination with the linear energy relations) can be used to understand the activity trends in transition metal catalyzed multistep organic reactions (dehydrogenation and hydrogenation reactions) as well as the hydrogen dissociation reaction as an initial step of catalytic hydrogenation reactions. Therefore, it can be concluded that the d-band model is qualitatively an important concept for understanding or predicting the reactivity trends in heterogeneous catalysis of transition metals for multistep organic reactions. As a first approximation, reactivity of a particular metal catalyst for the above organic reactions could be described by a single parameter, $\varepsilon_d - E_F$. In our previous study,[30] we have shown that there is a fairly good correlation between the d-band center and catalytic activity for more complicated reactions; the activity of transition metal-loaded SiO_2 catalysts for *N*-alkylation of aniline with amines shows a volcano-type dependence on the $\varepsilon_d - E_F$ value. These findings may open possibilities in the development of new catalysts without extensive trial-and-error experimental testing.

It is important to note that the d-band model in combination with Sabatier's principle is not a suitable method for quantitative description of the catalytic activity because the Sabatier reaction rate is the maximum rate that can be achieved under the assumption that all surface coverages are optimal. As established by Toulhoat and Raybaud,[8] use of DFT based activity descriptors combined with microkinetic models are effective method for the quantitative description of the catalytic activity.

CONCLUSION

We studied the correlations between the reaction rates and the $\varepsilon_d - E_F$ value of supported metal (M = Ag, Cu, Pt, Ir, Pd, Rh, Ru, Ni, and Co) catalysts for the following reactions: dehydrogenation of adsorbed 2-propanol and hydrogenation of adsorbed nitrobenzene under H_2 (as test reactions on metal surfaces), OH/OD exchange in a flow of D_2 (as a test reaction of H_2 dissociation on metal surfaces), liquid phase hydrogenation of nitrobenzene (as an organic reaction under realistic conditions). Generally, the activities showed volcano-type dependences on the ε_d-E_F value, indicating that the d-band model could be applicable to describing activity trends in multistep organic reactions.

ASSOCIATED CONTENT

Supporting Information

Further details are given in Figures S1−S4. This material is available free of charge via the Internet at http://pubs.acs.org.

AUTHOR INFORMATION

Corresponding Author

*E-mail: kshimizu@cat.hokudai.ac.jp. Fax: +81-11-706-9163.

Notes

The authors declare no competing financial interest.

REFERENCES

(1) Boudart, M. In *Handbook of Heterogeneous Catalysis*; Ertl, G., Knözinger, H., Weitkamp, J., Eds.; Wiley-VCH: Weinheim, Germany, 1997.
(2) Hammer, B.; Nørskov, J. K. *Adv. Catal.* **2000**, *45*, 71−129.
(3) Nørskov, J. K.; Bligaard, T.; Rossmeisl, J.; Christensen, C. H. *Nat. Chem.* **2009**, *1*, 37−46.
(4) Nørskov, J. K.; Abild-Pedersen, F.; Studt, F.; Bligaard, T. *Proc. Natl. Acad. Sci. U. S. A.* **2011**, *108*, 937−943.
(5) van Santen, R. A.; Neurock, M.; Shetty, S. G. *Chem. Rev.* **2010**, *110*, 2005−2048.
(6) Toulhoat, H.; Raybaud, P.; Kasztelan, S.; Kresse, G.; Hafner, J. *Catal. Today* **1999**, *50*, 629−636.
(7) Jacobsen, C. J. H.; Dahl, S.; Clausen, B. S.; Bahn, S.; Logadottir, A.; Nørskov, J. K. *J. Am. Chem. Soc.* **2001**, *123*, 8404−8405.
(8) Toulhoat, H.; Raybaud, P. *J. Catal.* **2003**, *216*, 63−72.
(9) Bligaard, T.; Nørskov, J. K.; Dahl, S.; Matthiesen, J.; Christensen, C. H.; Sehested, J. *J. Catal.* **2004**, *224*, 206−217.
(10) Nørskov, J. K.; Bligaard, T.; Hvolbaek, B.; Abild-Pedersen, F.; Chorkendorff, I.; Christensen, C. H. *Chem. Soc. Rev.* **2008**, *37*, 2163−2171.
(11) Cheng, J.; Hu, P.; Ellis, P.; French, S.; Kelly, G.; Lok, C. M. *J. Phys. Chem. C* **2008**, *112*, 1308−1311.
(12) Loffreda, D.; Delbecq, F.; Vigné, F.; Sautet, P. *Angew. Chem., Int. Ed.* **2009**, *48*, 8978−8980.
(13) Guernalec, N.; Geantet, C.; Cseri, T.; Vrinat, M.; Toulhoat, H.; Raybaud, P. *Dalton Trans.* **2010**, *39*, 8420−8422.
(14) Studt, F.; Abild-Pedersen, F.; Hansen, H. A.; Man, I. C.; Rossmeisl, J.; Bligaard, T. *ChemCatChem* **2010**, *2*, 98−102.
(15) Xing, B.; Pang, X.; Wang, G. *J. Catal.* **2011**, *282*, 74−82.
(16) Ruban, A.; Hammer, B.; Stoltze, P.; Skriver, H. L.; Nørskov, J. K. *J. Mol. Catal. A* **1997**, *115*, 421−429.
(17) Pallassana, V.; Neurock, M.; Hansen, L. B.; Hammer, B.; Nørskov, J. K. *Phys. Rev. B* **1999**, *60*, 6146−6154.
(18) Stamenkovic, V.; Mun, B. S.; Mayrhofer, K. J. J.; Ross, P. N.; Markovic, N. M.; Rossmeisl, J.; Greeley, J.; Nørskov, J. K. *Angew. Chem., Int. Ed.* **2006**, *45*, 2897−2901.
(19) Lu, C.; Lee, I. C.; Masel, R. I.; Wieckowski, A.; Rice, C. *J. Phys. Chem. A* **2002**, *106*, 3084−3091.
(20) Toyoda, E.; Jinnouchi, R.; Hatanaka, T.; Morimoto, Y.; Mitsuhara, K.; Visikovskiy, A.; Kido, Y. *J. Phys. Chem. C* **2011**, *115*, 21236−21240.
(21) Lima, F. H. B.; Zhang, J.; Shao, M. H.; Sasaki, K.; Vukmirovic, M. B.; Ticianelli, E. A.; Adzic, R. R. *J. Phys. Chem. C* **2007**, *111*, 404−410.
(22) Pallassana, V.; Neurock, M. *J. Catal.* **2000**, *191*, 301−317.
(23) Zheng, R.; Humbert, M. P.; Zhu, Y.; Chen, J. G. *Catal. Sci. Technol.* **2011**, *1*, 638−643.
(24) Kunimori, K.; Uchijima, T.; Yamada, M.; Matsumoto, H.; Hattori, T.; Murakami, Y. *Appl. Catal.* **1982**, *4*, 67−81.
(25) Zaki, M. I.; Hasan, M. A.; Pasupulety, L. *Langmuir* **2001**, *17*, 4025−4034.
(26) van Hardeveld, R.; Hartog, F. *Surf. Sci.* **1969**, *15*, 189−230.
(27) Shimizu, K.; Miyamoto, Y.; Satsuma, A. *J. Catal.* **2010**, *270*, 86−94.
(28) Tamura, M.; Shimizu, K.; Satsuma, A. *Appl. Catal., A* **2012**, *433−434*, 135−145.
(29) Bron, M.; Teschner, D.; Knop-Gericke, A.; Jentoft, F. C.; Krohnert, J.; Hohmeyer, J.; Volckmar, C.; Steinhauer, B.; Schlögl, R.; Claus, P. *Phys. Chem. Chem. Phys.* **2007**, *9*, 3559−3569.
(30) Shimizu, K.; Ohshima, K.; Tai, Y.; Tamura, M.; Satsuma, A. *Catal. Sci. Technol.* **2012**, *2*, 730−738.

NOTE ADDED AFTER ASAP PUBLICATION

After this paper was published on the Web August 7, 2012, a correction was made to author Kenichi Kon's name. The corrected version was reposted September 7, 2012.